American Mineralogist, Volume 95, pages 574–581, 2010

The incommensurately modulated structures of natural natrite at 120 and 293 K from synchrotron X-ray data

Alla Arakcheeva,[1] Luca Bindi,[2,*] Philip Pattison,[1,3] Nicolas Meisser,[4] Gervais Chapuis,[1] and Igor Pekov[5]

[1]Laboratoire de Cristallographie, École Polytechnique Fédérale de Lausanne, CH-1015 Lausanne, Switzerland
[2]Museo di Storia Naturale, Sezione Mineralogia, Università di Firenze, Via La Pira 4, I-50121 Firenze, Italy
[3]Swiss-Norwegian Beamline, ESRF, BP-220, F-38043 Grenoble Cedex, France
[4]Musée de géologie, Lausanne University, UNIL-Dorigny, CH-1015 Lausanne, Switzerland
[5]Geological Faculty, Moscow State University, Vorobievi Gori, Moscow, 1119992 Russia

Abstract

The incommensurately modulated structure of the mineral natrite has been refined for the first time. Two single-crystal grains, *Lv* and *Kh*, from two different occurrences [Mt. Karnasurt, Lovozero massif (*Lv*), Kola peninsula, Russia, and the pegmatite of Mt. Koashva, Khibiny massif (*Kh*)], have been investigated at 293 and 120 K using synchrotron X-ray data. The average structures of both minerals are identical and the basic features of the structural modulations are similar to the synthetic γ-Na_2CO_3 phase previously published. The γ (incommensurate) → δ (lock-in) phase transition reported at low temperature for the synthetic compound was not observed down to 120 K in natural natrite. Crystal-chemical aspects, especially about the second coordination sphere for the carbon atoms, are examined to explain the different structural behaviors observed at low temperature. The possible role played by the minor isomorphous substitutions in natural natrite specimens is also discussed.

Keywords: Incommensurate structure, natrite, superspace, synchrotron X-ray data

Introduction

Natrite, Na_2CO_3, is a rare mineral, an endogenous high-temperature anhydrous carbonate, which was discovered in the Lovozero and Khibiny alkaline massifs, Kola Peninsula, Russia, and described as a new mineral in 1982 (Khomyakov 1982). From a comparison of the X-ray powder diffraction pattern of synthetic γ-Na_2CO_3 (Brouns et al. 1964) with that obtained from natrite, Khomyakov (1982) assumed the structures to be identical. The γ-Na_2CO_3 phase of the synthetic compound is a well-known, incommensurately modulated phase. This compound shows several temperature-dependent phase transitions: α-Na_2CO_3 (hexagonal; 756–972 K) → β-Na_2CO_3 (monoclinic; 605–751 K) → γ-Na_2CO_3 (incommensurate, monoclinic; below 605 K) → δ-Na_2CO_3 (commensurately modulated, lock-in phase, monoclinic; the lowest-temperature phase). In this sequence, the highest-temperature hexagonal modification (Fig. 1) undergoes a monoclinic distortion that is accompanied by a change in the second coordination sphere of C from coordination number (CN) = 3 to CN = 7 (Arakcheeva and Chapuis 2005). The incommensurately modulated structure of γ-Na_2CO_3 at 295 K was solved by van Aalst et al. (1976) and later refined with higher accuracy using X-ray single-crystal diffraction data [Dušek et al. 2003: *C*2/*m*(α0γ)0s; *a* = 8.920(7), *b* = 5.245(5), *c* = 6.050(5) Å, β = 101.35(8)°, **q** = 0.182(1)**a*** + 0.322(1)**c***]. Dušek et al. (2003) also solved the commensurately modulated structure of the δ phase at 110 K [*C*2/*m*(α0γ)0s; *a* = 8.898(7), *b* = 5.237(5), *c* = 5.996(5) Å, β = 101.87(8)°, **q** = 1/6**a*** + 1/3**c***], and they reported the γ → δ transition at 170 K, which is higher than the value of 130 K obtained earlier by de Pater and Helmholdt (1979) on the basis of neutron diffraction experiments. Satellite reflections pointing to an incommensurately modulated structure were also observed during the single-crystal investigation of natrite from Khibiny at 295 K (Zubkova et al. 2002). However, the satellites were not measured, and the authors refined only the average structure of this mineral sample. Therefore, the crystal structure of the mineral natrite is still lacking a complete characterization.

The main aim of the present work is to characterize the incommensurately modulated structure of natrite at room temperature,

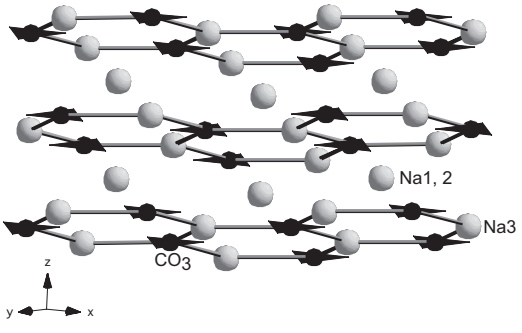

Figure 1. Structure of the hexagonal highest-temperature modification of Na_2CO_3.

* E-mail: luca.bindi@unifi.it

293 K, and at 120 K, a temperature lower than that previously reported for the $\gamma \rightarrow \delta$ phase transition. The anhydrous sodium carbonate, Na_2CO_3, is a strong hydrophilic material: with atmospheric water and CO_2 it slowly transforms into hydrates and hydrogeno-carbonates [e.g., thermonatrite, $Na_2CO_3 \cdot H_2O$, natron $Na_2CO_3 \cdot 10H_2O$, trona $Na_3(CO_3)(HCO_3) \cdot 2H_2O$]. Hence, only very small, suitable single-crystal grains could be selected for the X-ray measurements. Under these circumstances, the use of synchrotron radiation is mandatory.

Before concluding this introduction, we present a brief review of the superspace concept.

The first solution of the γ-Na_2CO_3 structure by de Wolff and coworkers (van Aalst et al. 1976) was at the origin of the introduction of the superspace formalism for the description of modulated structures, which are characterized by the presence of satellite reflections in their diffraction pattern. If the periodicity of the satellites is incommensurate with the periodicity of the reciprocal lattice parameters, the corresponding structure is incommensurately modulated or aperiodic (e.g., γ-Na_2CO_3). In the other case, the structure is commensurately modulated, often called a superstructure (e.g., δ-Na_2CO_3). To recover the periodicity of incommensurately modulated structures, de Wolff extended their descriptions in higher dimensional space, i.e., superspace. For Na_2CO_3, it is sufficient to extend its description in four dimensions, more precisely (3+1)-dimensions, (3+1)D. The real structures can be recovered by rational 3D sections of the higher dimensionally periodic structures (commensurately modulated structures) or irrational 3D sections (incommensurately modulated structures). Figure 2 illustrates the principle of the superspace concept for a (1+1)D structure. The symmetry of structures described in superspace is also well characterized by superspace groups, which are tabulated similar to the space groups (Janssen et al. 2004). Many different cases of both commensurately and incommensurately modulated structures, including Na_2CO_3, are theoretically considered by Janssen et al. (2007). Useful practical information, such as the relations between (3+1)D and 3D groups for commensurately modulated structures, an applet to find a superspace model for a set of related structures by simulating the diffraction pattern for each structure, a database that provides information concerning groups of symmetry of arbitrary dimensions, potential transformations of (3+1)D Bravais classes into 3D classes for commensurate modulation, and other aspects of the superspace approach, is currently available from the website developed by Laboratoire de Cristallographie, École Polytechnique Fédérale de Lausanne (http://lcr.epfl.ch/page55041.html).

Experimental methods

Two different samples of natrite have been used for the structural investigation. The first, hereafter labeled *Lv*, is a part of the type material collected and described by Khomyakov (1982) in the Lovozero alkaline massif (Mt. Karnasurt) and consists of natrite, partially altered on the surface to trona, with minor villiaumite, NaF. The second, hereafter labeled *Kh*, is a part of the type material collected by one of the authors (I.P.) in the Khibiny alkaline massif (Mt. Koashva) and then donated to the Musée cantonal de géologie of Lausanne, and consists of natrite, partially altered on the surface to trona and thermonatrite and contains inclusions of dark-brown lamellae of lomonosovite, $Na_2Ti_2Si_2O_9Na_3PO_4$, olive-green prisms of aegirine, $NaFeSi_2O_6$, and colorless bright prisms of manganoan pectolite, $Na(Ca_{1.73}Mn_{0.27})[HSi_3O_9]$ previously studied by Arakcheeva et al. (2007). Both samples are housed in the collection of the Musée cantonal de géologie of Lausanne (catalog numbers: MGL 58960 and MGL 92266 for *Lv* and *Kh*, respectively). Detailed information about the occurrence of *Lv* and *Kh* crystals was reported by Khomyakov (1982) and Zubkova et al. (2002), respectively.

Chemical composition

Chemical analyses of both *Lv* and *Kh* were carried out by means of a scanning electron microscope, CamScan MV2300, coupled with an Inca X-sight energy dispersive spectrometer from Oxford Instruments (Institute of Geology and Paleontology, Faculté des géosciences et de l'environnement, University of Lausanne). Analyses of 100 s each were conducted using a tightly focused beam scanned over a surface of about 20 μm^2, an accelerating voltage of 20 kV, a sample current of 40 μA, and vacuum of $1.5 \cdot 10^{-5}$ Pa. The following X-ray lines (and analytical standards)

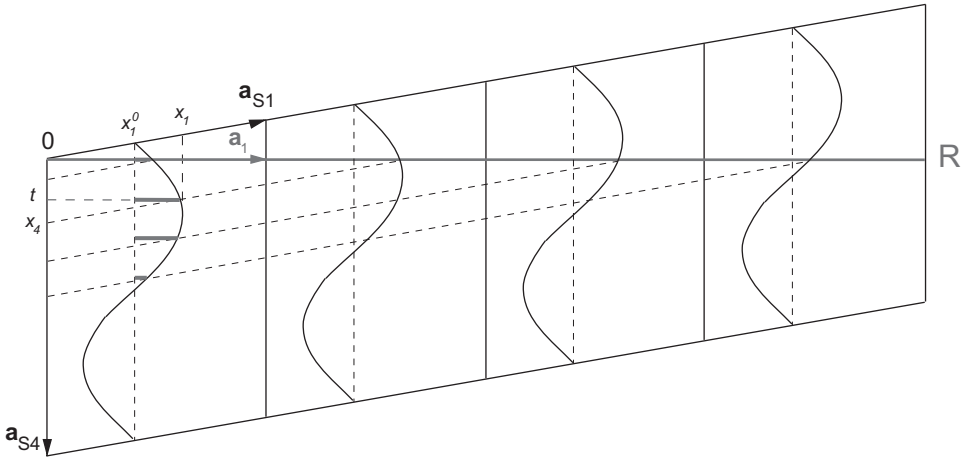

Figure 2. Illustration of the mapping of a periodic (1+1)D structure in superspace along the line R (the real space). $\mathbf{a}_{S1}$ and $\mathbf{a}_{S4}$ are translation vectors along the x_1 and, respectively, x_4 (and t) axes of the (1 + 1)D superspace; $\mathbf{a}_1$ is the lattice constant. Curves specify a periodic displacement of atomic coordinate x_1 from the average value x^0_1 for one atom. Intersections of these curves with R give the positions of the atom in real 1D space, which is aperiodic. Line R can be displaced vertically and its displacement is expressed by the variable t. The corresponding intersections represent different portions of the 1D structure. In general, t is the variable of choice to characterize atomic displacements as a function of x_i ($1 \leq i \leq 3$). The difference between t and x_4 is indicated in the figure. Similar curves as functions of t can also correspond to ADPs and occupancy of an atom as well as to an interatomic distance.

were used: Na*K*α (NaCl) and Ca*K*α ($CaCO_3$). Some analyzed parts of crystals show no impurities or only minor content of Ca, corresponding to the following formula: $Na_{2-x}Ca_xCO_3$ with $0.00 < x < 0.04$. Other elements such as Mg, Si, Al, F, and P, if present, are below the detection limit (<0.05 wt%). The presence of Li was checked qualitatively using a Krüss flame spectrometer (Musée géologique, Lausanne), but it appears that this element is absent in both samples *Lv* and *Kh*.

Synchrotron X-ray diffraction experiment

The crystals were hand picked from the mineral samples immersed in paraffin oil. The original pieces, 1–2 mm in size, were broken into fragments, and crystals of about 0.05 and 0.03 mm in average size were selected for *Lv* and *Kh*, respectively. They were mounted onto glass rods with paraffin oil. The selected fragments were transparent, whereas most of the original material was milky white in color. Several other crystals were tested, but most of them showed strong powder rings in their diffraction patterns.

The prepared samples of *Lv* and *Kh* were mounted onto the spindle axis of a MarResearch Image Plate Detector System, and the data collection was carried out at 293 and 120 K for each of them. Temperature control was achieved using a cooled-nitrogen gas cryostream supplied by an Oxford Cryosystems low-temperature device. The MAR345 detector is installed on the Swiss-Norwegian Beam Line (BM1A) at the ESRF. A wavelength of 0.7100 Å was selected using a Si(111) monochromator. A combination of a sagittally bent monochromator and a curved mirror provided a focal spot of approximately 0.5 × 0.5 mm. Secondary slits on the MAR345 base were used to define a beam cross section of 0.3 × 0.3 mm at the sample position. The sample-to-detector distance was 130 mm, and a total of 359 images for *Lv* and 348 for *Kh* were collected with a rotation of 1° per image using the full 345 mm active diameter of the image plate. The data were collected in dose mode, with an approximate exposure time of 4 s/frame. The detector geometry and scattering power gave a maximum 2θ angle of 53° with a maximum resolution of 0.796 Å. The data collection obtained for *Lv* was limited to this resolution due to its smaller size. Moreover, splitting of all reflections in the data collection obtained for *Lv* at 120 K pointed to a broken crystal, and only the room-temperature data were used for this sample. Because the *Kh* sample scattered well, further data sets on the same crystal were collected at 293 and 120 K, using a combination of an Oxford Diffraction KM6 multi-axis diffractometer and a CCD detector yielding data with a maximum 2θ angle of 72° and a resolution of 0.603 Å.

The indexing and integration of the diffraction data were carried out with the CrysAlis RED software package from Oxford Diffraction (Version 1.171.28). The diffraction patterns revealed satellite reflections up to the third order for *Kh* (at both 293 and 120 K) and second order for *Lv* relating to the main reflections indexed in a monoclinic cell with approximate parameters: $a = 8.8$, $b = 5.2$, $c = 6.0$ Å, $\beta = 101°$. The satellites could be indexed with an approximate modulation vector $\mathbf{q} = 0.18\mathbf{a}^* + 0.32\mathbf{c}^*$. They were refined for each experimental data set using the NADA option in CrysAlis. No low-temperature incommensurate-commensurate phase transition ($\gamma \rightarrow \delta$ phase transition) was observed for *Kh*. Experimental details, values of the refined unit-cell parameters, and the **q**-vectors are listed in Table 1.

Superspace refinements of the structures

All calculations related to the structure refinement were performed with the Jana2000 system of programs (Petříček et al. 2000). The experimental data collections obtained for *Kh* at 293 and 120 K and that obtained for *Lv* at 293 K revealed identical systematic extinctions (*hklm*: $h + k = 2n$; *h*0*lm*: $m = 2n$), which unequivocally define the $C2/m(\alpha 0 \gamma)0s$ superspace group. Because of the similarity of both the unit-cell values and incommensurate **q**-vectors (Table 1) to those of the γ-Na_2CO_3 synthetic compound (Dušek et al. 2003) and because the same superspace group describes both, we used the fractional coordinates of atoms reported for γ-Na_2CO_3 as a starting model for the average structure in our refinements.

The experimental data sets, *Kh* (293 K), *Kh* (120 K), and *Lv* (293 K), were treated with the following procedure for the structural study. The fractional coordinates of 6 atoms (Na1, Na2, Na3, C, O1, and O2) were refined in the $C2/m(\alpha 0 \gamma)0s$

Table 1. Experimental details for the selected natrite crystals

	Crystal data		
Mineral	*Kh*, 120 K	*Kh*, 293 K	*Lv*, 293 K
Cell setting, superspace group	Monoclinic, $C2/m(\alpha 0 \gamma)0s$	Monoclinic, $C2/m(\alpha 0 \gamma)0s$	Monoclinic, $C2/m(\alpha 0 \gamma)0s$
a, *b*, *c* (Å)	8.825(2), 5.194(3), 5.953(2)	8.851(2), 5.24(2), 6.021(2)	8.8818(17), 5.235(10), 6.0455(11)
β (°)	101.83(3)	101.08(2)	101.464(12)
V (Å³)	267.08(18)	274.00(15)	275.49(5)
Z	2	2	2
Modulation wave vector	$\mathbf{q} = 0.17951(1)\mathbf{a}^* + 0.31905(1)\mathbf{c}^*$	$\mathbf{q} = 0.18370(1)\mathbf{a}^* + 0.31116(1)\mathbf{c}^*$	$\mathbf{q} = 0.1834(1)\mathbf{a}^* + 0.3207(1)\mathbf{c}^*$
Data collection			
Radiation type, λ (Å)	Synchrotron, 0.71	Synchrotron, 0.71	Synchrotron, 0.71
No. reflections for cell parameters	14879	15528	9905
θ range (°)	2.54–35.90	2.46–36.48	2.52–26.54
Temperature (K)	120	293	293
Crystal form, color	Irregular, colorless	Irregular, colorless	Irregular, colorless
Crystal sizes (mm)	0.07 × 0.05 × 0.03	0.07 × 0.05 × 0.03	0.05 × 0.035 × 0.02
Diffractometer	Oxford Diffraction KM6	Oxford Diffraction KM6	MAR345
Data collection method	CCD area detector	CCD area detector	MAR IP
Absorption correction method	SADABS	SADABS	SADABS
No. of measured reflections	14879	15528	9905
No. of independent reflections	3587	2544	1475
No. of observed reflections	1750	1042	1071
No. of main reflections	544	392	315
No. of satellite reflections (1st-order, 2nd-order, 3rd-order)	3043 (959, 1123, 961)	2152 (673, 803, 676)	1160 (519, 641, 0)
Criterion for observed reflections	$I > 3\sigma(I)$	$I > 3\sigma(I)$	$I > 3\sigma(I)$
R_{int}	0.0916	0.1493	0.0915
Range of *h*, *k*, *l*, *m*	$-12 \rightarrow h \rightarrow 12$, $-8 \rightarrow k \rightarrow 8$, $-9 \rightarrow l \rightarrow 9$, $-3 \rightarrow m \rightarrow 3$	$-13 \rightarrow h \rightarrow 12$, $-8 \rightarrow k \rightarrow 8$, $-10 \rightarrow l \rightarrow 10$, $-3 \rightarrow m \rightarrow 3$	$-11 \rightarrow h \rightarrow 11$, $-6 \rightarrow k \rightarrow 6$, $-8 \rightarrow l \rightarrow 8$, $-2 \rightarrow m \rightarrow 2$
Refinement			
Refinement on	*F*	*F*	*F*
S	2.00	1.55	2.47
R, *wR* (observed main reflections)	0.0511, 0.0636	0.0522, 0.0479	0.0507, 0.0474
R, *wR* (observed 1st-order satellite reflections)	0.0598, 0.0740	0.0641, 0.0553	0.0656, 0.0428
R, *wR* (observed 2nd-order satellite reflections)	0.0742, 0.0934	0.0807, 0.0864	0.1079, 0.1014
R, *wR* (observed 3rd-order satellite reflections)	0.0843, 0.0904	0.0821, 0.0850	–
R, *wR* (all observed reflections)	0.0608, 0.0756	0.0619, 0.0565	0.0649, 0.0565
No. of reflections and parameters used in refinement	3587, 204	2544, 214	1475, 151
Weighting scheme	$w = 1/[\sigma^2(F) + 0.000025F^2]$	$w = 1/[\sigma^2(F) + 0.000025F^2]$	$w = 1/[\sigma^2(F) + 0.000025F^2]$
(Δ/σ_{max})	0.0006	0.0008	0.0008
$\Delta\rho_{max}$, $\Delta\rho_{min}$ (*e*Å^{-3})	0.96, –0.83	0.76, –0.70	0.84, –0.79

Note: Source of atomic scattering factors: *International Tables for X-ray Crystallography* (1992, Vol. C, Tables 4.2.6.8 and 6.1.1.1.).

TABLE 2. Fractional atomic coordinates, occupations and equivalent isotropic displacement parameters in natrites in comparison with the synthetic γ-Na_2CO_3 (Dušek et al. 2003)

Atom	*Kh*, 120 K	*Kh*, 293 K	*Lv*, 293 K	Synthetic γ-Na_2CO_3*
		Na1		
Occupation	0.976(4) Na	0.977(1) Na	0.978(5) Na	0.989(2)
x	0	0	0	0
y	0	0	0	0
z	0	0	0	0
U_{eqv} (Å²)	0.0117(3)	0.0191(4)	0.0189(4)	0.01731(11)
		Na2		
Occupation	0.987(4) Na	0.987(1) Na	0.975(5) Na	0.990(2)
x	0	0	0	0
y	0	0	0	0
z	½	½	½	½
U_{eqv} (Å²)	0.0117(8)	0.0197(3)	0.0182(4)	0.01673(11)
		Na3		
Occupation	0.977(3) Na	0.977(1) Na	0.970(5) Na	0.990(2)
x	0.17101(6)	0.17036(9)	0.17065(8)	0.17055(4)
y	½	½	½	½
z	0.74766(10)	0.74816(13)	0.74801(12)	0.74801(6)
U_{eqv} (Å²)	0.0155(2)	0.0271(3)	0.0264(4)	0.02554(10)
		C		
Occupation	1	1	1	1
x	0.16446(13)	0.16441(17)	0.16426(18)	0.16446(7)
y	½	½	½	½
z	0.2492(2)	0.2492(2)	0.2491(2)	0.24914(10)
U_{eqv} (Å²)	0.0103(3)	0.0145(4)	0.0133(5)	0.01155(13)
		O1		
Occupation	1	1	1	1
x	0.10211(9)	0.10178(10)	0.10165(11)	0.10159(5)
y	0.29314(14)	0.29423(19)	0.29451(18)	0.29384(7)
z	0.28695(13)	0.28557(15)	0.28529(13)	0.28535(7)
U_{eqv} (Å²)	0.0186(3)	0.0310(4)	0.0283(5)	0.02607(12)
		O2		
Occupation	1	1	1	1
x	0.28945(11)	0.28986(14)	0.28932(15)	0.28987(6)
y	½	½	½	½
z	0.17451(17)	0.1776(2)	0.1776(2)	0.17757(11)
U_{eqv} (Å²)	0.0159(3)	0.0271(6)	0.0257(4)	0.02274(14)

Notes: * The values of the occupation of the Na position has been obtained from the additional refinement of the synthetic γ-Na_2CO_3. Fourier amplitudes of the displacive modulation functions are available from the CIF files[1] submitted for *Kh* (120 K), *Kh* (293 K), and *Lv* (293 K).

superspace group with both main and satellite reflections. The refined parameters (Table 2) obtained for the *Kh* and *Lv* modulated structures appeared to be identical to those reported for synthetic γ-Na_2CO_3 (295 K; Dušek et al. 2003) within 1–4 standard uncertainties (su) at 293 K and 1–10 su at 120 K. The harmonics of the displacive modulation were introduced gradually into the refinement for all atoms. After every set of iterations, the quality of the results was checked using the atomic modulation functions and the x_4x_1, x_4x_2, and x_4x_3 sections of the Fourier synthesis of electron density calculated for each atom. The *R*-factors smoothly converged to lower and stable values following the introduction of new harmonic terms. For each atom, the number of harmonics was increased until the modulation function reproduced optimally the electron density in all the Fourier synthesis sections mentioned above. As satellites could be measured only to the second order for the *Lv* crystal, the number of displacive modulation harmonics (3 for Na1, Na2, C, and O1; 4 for Na3; 2 for O2) included for the atoms is less than the number of the corresponding harmonics (4 for Na1, Na2, C, and O1; 5 for Na3; 3 for C and O2) in the *Kh* structures, which have been experimentally characterized with satellites up to the third order. The most intense displacive modulations of all atoms correspond to the x_4x_2 section (Fig. 3).

Following the refinement of the atomic displacive modulations, the atomic displacement parameters (ADP) of all atoms were still higher than expected in comparison with those of the synthetic γ-Na_2CO_3 (Dušek et al. 2003) and the values of the *R*-factors on the satellite reflections were higher than 0.1. Including ADP harmonic modulations for all atoms improved both the *R*-factors and values of ADPs. Again, the number of harmonics incorporated in the refinement for modulation of ADP is different for all three structures presented here: in *Kh* (293 K): 2 for C, Na1, and Na2, 3 for Na3, 4 for O1 and O2; in *Kh* (120 K): 2 for C, Na1, and Na2, 3 for Na3 and O2, 4 for O1; in *Lv* (293 K): 1 for Na2, 2 for Na1, Na3, O1, and O2, and none for C. Modulations of the equivalent isotropic ADP, U_{eqv}, are shown in Figure 4 for the studied structures in comparison with γ-Na_2CO_3 (Dušek et al. 2003).

As shown in Figure 4, the U_{eqv} parameters of Na2 and Na3 atoms show an unusually large magnitude of modulation in the *Lv* structure in comparison with γ-Na_2CO_3 (Dušek et al. 2003). Thus, individual occupational modulations were refined for each Na atom in *Lv*. Indeed, a partial substitution of Na^+ by a lighter element and/or vacancies could be postulated. For this reason, we decided to refine an unconstrained site occupancy for the Na sites [Na vs. □ (structural vacancy)]. As a result of this refinement of *Lv*, the wR_{obs} and *S* values decreased from 0.0603 to 0.0565 and from 2.53 to 2.47, respectively. The resulting characteristics of the Na-position occupation modulations are presented in Figure 5 (right). Comparison of the U_{eqv} modulations obtained for the Na-positions fully occupied by Na (*Lv* in Fig. 5) to those partially occupied by Na (Fig. 5, right-top) shows that the inclusion of some vacancy contribution decreases the magnitude of the U_{eqv} modulations. The same procedure was applied to both the *Kh* (293 K) and *Kh* (120 K) structures. Here also, the refined values of the occupancy at the Na sites were slightly <1 (Fig. 5, left and middle) without affecting other atomic parameters or the overall quality of the refinement. For *Kh* (120 K), for instance, wR_{obs} decreased only from 0.0756 to 0.0748, while $S = 2.00$ remained unchanged. A possible interpretation of the lower occupation of the Na-positions in both *Lv* and *Kh* structures will be given below.

The main characteristics of the final refinements are listed in Table 1. The occupation of the Na-positions and the average values of U_{eqv} are given in Table 2 for all the atoms, along with the fractional coordinates of the atoms. The Na-O

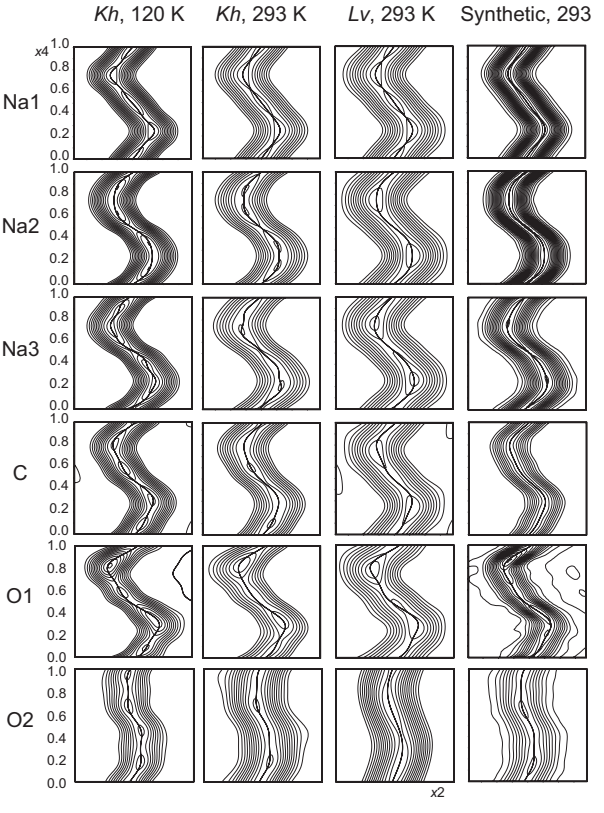

FIGURE 3. The x_2x_4 sections of the Fourier synthesis calculated in the vicinity of different atoms in Na_2CO_3 structures. The step between two lines is 1 eÅ^{-3} for O and C and 2 eÅ^{-3} for Na. The central bold line corresponds to the refined atomic positions in each section.

[1] Deposit item AM-10-018, CIFs. Deposit items are available two ways: For a paper copy contact the Business Office of the Mineralogical Society of America (see inside front cover of recent issue) for price information. For an electronic copy visit the MSA web site at http://www.minsocam.org, go to the *American Mineralogist* Contents, find the table of contents for the specific volume/issue wanted, and then click on the deposit link there.

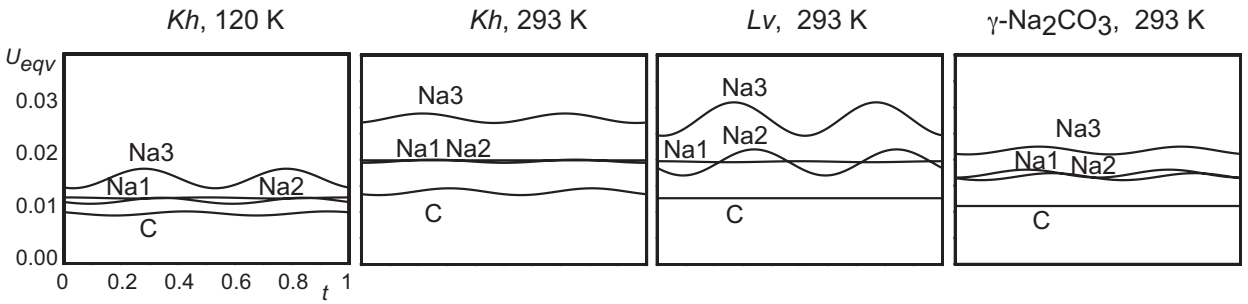

FIGURE 4. Modulations of the isotropic displacement parameters, U_{eqv}, of Na and C in their fully occupied positions plotted along the *t* axis. The magnitude of the modulation is unusually high for Na in *Lv* at 293 K (see text for explanation).

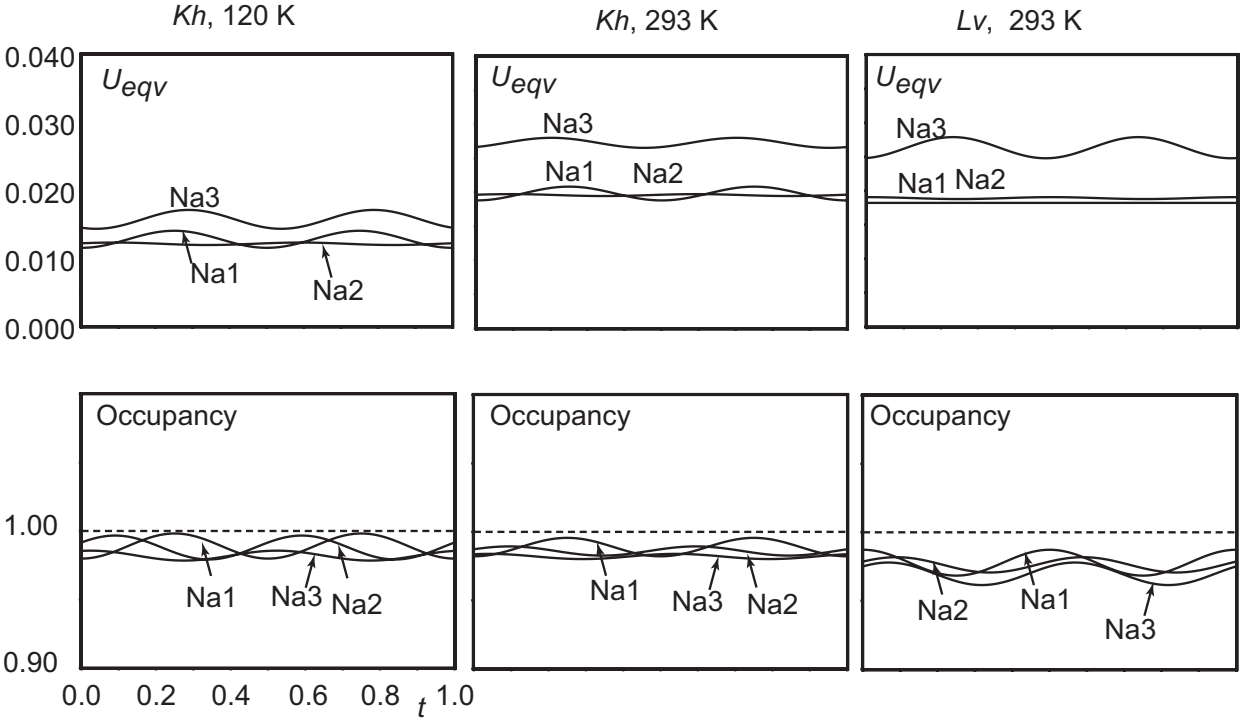

FIGURE 5. Modulations of occupancy and corresponding modulations of the isotropic displacement parameters, U_{eqv}, of Na plotted along the *t* axis. The dashed line shows 100% occupancy for comparison.

and C-Na distances are plotted in Figure 6 as functions of the fourth axis, *t*. The modulation characteristics of the CO_3 group along *t* is shown in Figure 7.

RESULTS AND DISCUSSION

The average structure of natrite can be globally described as graphite-like layers formed by Na3 and CO_3 ions, stacked along the *c* axis (Fig. 1). Additional Na1,2 octahedral-ions are located in the pseudo-hexagonal channels (van Aalst et al. 1976; Zubkova et al. 2002; Dušek et al. 2003). The face-sharing Na1,2 octahedra form columns, which are connected by CO_3 triangles along [010] and [100]. As can be deduced from Figure 6, the CN of Na1,2 can be better described as 4+2, where 4 distances are shorter than 2.3 Å, and 2 distances are about 2.4 Å. The Na3 site has been reported as 7+2-fold coordinated with 7 Na-O distances in the range 2.584(1)–2.669(1) Å and two elongated Na-O distances at 2.942(1) Å (Zubkova et al. 2002). It is evident from the modulation of the Na3-O distances (Fig. 6) that eight oxygen atoms are always present near Na3 (in the range 2.35–2.9 Å) without any preference for CN = 7. Therefore, the coordination number of Na3 is equal to 8.

The modulated structure observed for natural natrite at room temperature closely resembles that of the γ phase of synthetic Na_2CO_3 (van Aalst et al. 1976; Dušek et al. 2003), which has been thoroughly discussed by de Wolff and Tuinstra (1986). For this reason, we shall focus on the differences between the low-temperature structural behavior observed in natrite (this study) and in synthetic Na_2CO_3 (Dušek et al. 2003).

The value of the coefficients of the modulation vector α and γ measured at room temperature [$\alpha = 0.18370(1)$, $\gamma = 0.31116(1)$ and $\alpha = 0.1834(1)$, $\gamma = 0.3207(1)$ for *Kh* and *Lv*, respectively] are close to the values determined for the incommensurate γ phase of synthetic natrite [$\alpha = 0.182(1)$ and $\gamma = 0.322(1)$, Dušek et al.

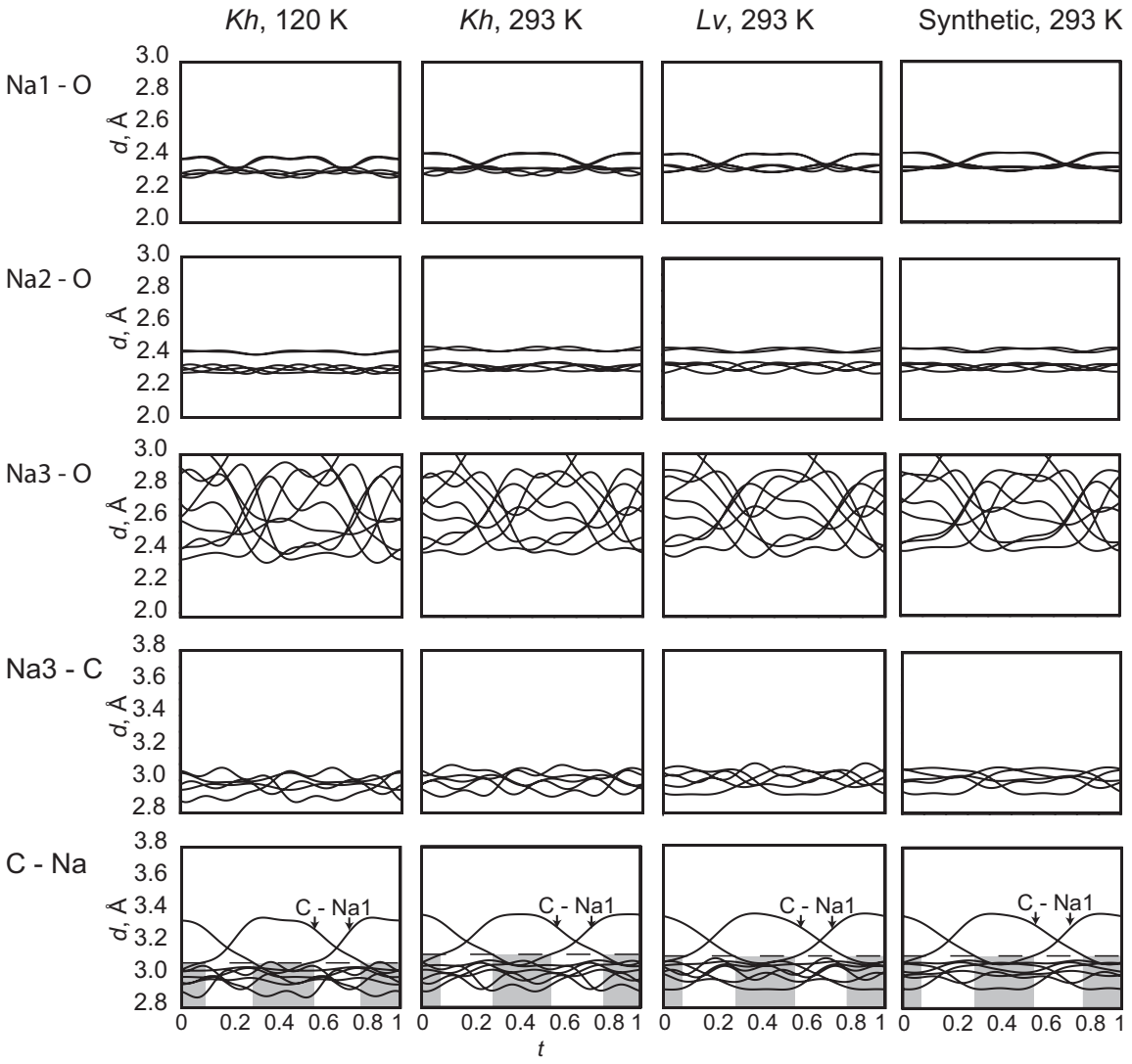

FIGURE 6. Modulations of the interatomic distances along the *t* axis in the indicated Na_2CO_3 structures. In the C-Na vs. *t* plots, the gray areas mark the regions with 7 Na atoms in the 3.1 Å (3.05 Å) vicinity of each C at 293 K (120 K).

(2003)]. This is not surprising as the chemical composition is nearly identical to that of the pure Na_2CO_3 end-member. Notwithstanding, strong differences with respect to synthetic natrite are found if the temperature dependence of the coefficients of the modulation vector (i.e., α and γ values) is considered. Indeed, for the natural *Kh* crystal, α decreases from 0.18370(1) at room temperature to 0.17951(1) at 120 K and γ increases from 0.31116(1) at room temperature to 0.31905(1) at 120 K. In synthetic Na_2CO_3 (Dušek et al. 2003), however, within a comparable temperature range, α decreases from 0.182(2) to the commensurate value 1/6 and γ increases from 0.322(1) to the commensurate value 1/3, thus indicating the stabilization of the lock-in low-temperature commensurate δ-phase. However, the reason for the differences between natural and synthetic natrite remains unclear. By analogy with other minerals exhibiting incommensurate structures (e.g., melilite-group minerals, Bindi et al. 2001 and references therein), we can speculate that the commensurate structure is not stabilized in natural natrite at low temperature because of the presence of minor substitutions at the Na and/or C structural sites. Indeed, as reported above, we observed in both the structures of *Kh* and *Lv* a site scattering amplitude lower than 11 units (Na) for the Na sites. For this reason, we have postulated four different substitution mechanisms that could be responsible for the different behavior of the modulated structure of natrite: (1) $Mg^{2+} + \square \rightarrow Na^+$ at the Na sites; (2) $C^{4+} + \square \rightarrow Na^+$ at the Na sites; (3) $Mg^{2+} \rightarrow Na^+$ at the Na sites and $B^{3+} \rightarrow C^{4+}$ at the C sites; and (4) $H^+ \rightarrow Na^+$ at the Na sites. The remaining mechanisms involving the presence of Li or K replacing Na were already discarded by virtue of the chemical tests that were carried out. Hypotheses 1, 2, and 3 were ruled out because they appeared extremely unlikely in mineralogical terms. Indeed, if the $C^{4+} \rightarrow Na^+$ substitution was improbable in terms of ionic radii, the other substitution mechanisms are very unlikely to be found in natural carbonates. For this reason, we focused our attention on the last mechanism, i.e., $H^+ \rightarrow Na^+$ replacement at the Na sites. This kind of cation substitution is indeed corroborated by the

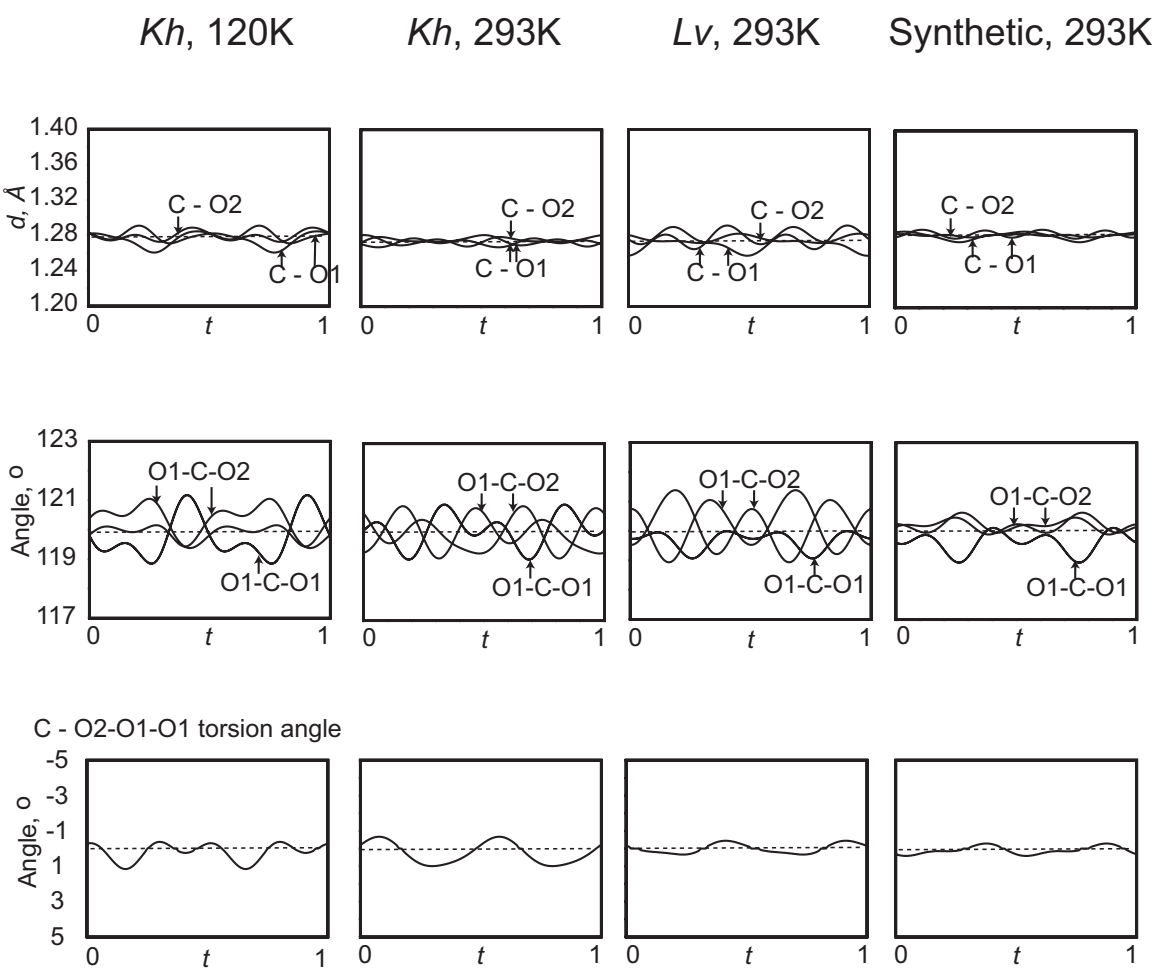

FIGURE 7. Characteristics of the CO_3-group geometry in the indicated Na_2CO_3 structures.

existence of the mineral nahcolite, $NaHCO_3$, which shows strong analogies with natrite. This mineral exhibits a crystal structure very similar to natrite (Sass and Scheuerman 1962) with the main differences being: (1) a graphite-like layer consisting of CO_3 groups and H, where the original Na3 structural site of natrite is replaced by H (however, the hydrogen atoms, although in the layer, are not exactly in the Na3 position), and (2) the CO_3 groups are perpendicular to the layer (i.e., not in the layer as in natrite). Thus, if we take into account the refined occupancy values at the Na sites obtained at room temperature for both *Kh* and *Lv* crystals (Table 2) together with the fact that a nahcolite component may be incorporated in their structures, the following chemical formulae are obtained: $(Na_{1.956}H_{0.044})CO_3$ and $(Na_{1.942}H_{0.058})CO_3$ for *Kh* and *Lv*, respectively. Nevertheless, if minor amounts of H replace Na at the Na sites, it does not affect the geometry of the polyhedra. Indeed, the mean bond distances for the Na sites (Table 3) are similar to those observed for the synthetic γ-phase of Na_2CO_3 (Dušek et al. 2003). On the other hand, some considerations can be made about the second coordination sphere of the carbon atoms. Arakcheeva and Chapuis (2005) pointed out the prominent role of the C-Na interactions [increase of the number of Na ions in the vicinity of C atoms, i.e., the coordination number (CN) of C in the second coordination sphere] in the stabilization of the different modulated structures in synthetic natrite. These authors observed that by decreasing temperature, some dramatic changes occur in the structure between non-O atoms, which are associated with the phase transformations. In detail, Arakcheeva and Chapuis (2005) established a systematic increase in the second coordination sphere of the C atoms as 3 → 4 → 5 → 6–7 (with a prevalence of the regions being sixfold coordinated) → 7 Na atoms, which fits the α → β → γ′ (predicted by Arakcheeva and Chapuis 2005) → γ → δ phase transitions observed for this synthetic compound. In this light, it does appear that in the low-temperature commensurate lock-in phase (δ phase), the second coordination sphere of C atoms is always characterized by seven Na sites. We observed the same structural behavior for the room-temperature incommensurate γ phase of natural natrite (Table 3; Fig. 6), which is characterized by a CN of the second-coordination sphere for the C atoms of 6–7. However, some differences can be highlighted for the 120 K crystal structure of the *Kh* crystal. Indeed, the CN of the C atoms in the second coordination sphere is still characterized by six and seven Na atoms (as in the room-temperature γ phase), but the regions coordinated by 7 atoms are larger along the *t* axis

TABLE 3. Interatomic distances (Å) in the modulated structures of natrites in comparison with the synthetic γ-Na_2CO_3 (Dušek et al. 2003)

	Kh, 120 K			*Kh*, 293 K			*Lv*, 293 K			Synthetic γ-Na_2CO_3		
	average	minimal	maximal	average	minimal	maximal	average	minimal	maximal	average	minimal	maximal
Na1-O1 x4	2.350(7)	2.284(7)	2.441(10)	2.374(10)	2.328(7)	2.447(14)	2.375(9)	2.318(8)	2.431(9)	2.377(2)	2.334(2)	2.434(2)
Na1-O2 x2	2.312(7)	2.284(6)	2.346(3)	2.320(9)	2.274(16)	2.368(16)	2.338(2)	2.315(2)	2.364(2)	2.340(2)	2.3185(18)	2.3616(18)
Na2-O1 x4	2.30(2)	2.26(3)	2.33(3)	2.316(9)	2.277(12)	2.355(8)	2.326(9)	2.282(9)	2.356(9)	2.326(3)	2.296(3)	2.351(3)
Na2-O2 x2	2.41(3)	2.35(5)	2.46(4)	2.426(7)	2.4142(17)	2.444(11)	2.4288(19)	2.4132(18)	2.4445(19)	2.4346(17)	2.4164(16)	2.4466(16)
Na3-O1	2.908(8)	2.585(8)	3.220(8)	2.952(11)	2.625(11)	3.239(11)	2.959(15)	2.614(15)	3.239(15)	2.964(3)	2.647(3)	3.244(3)
Na3-O1	2.617(8)	2.353(8)	2.940(8)	2.619(11)	2.382(10)	2.889(11)	2.626(15)	2.371(15)	2.893(15)	2.636(3)	2.402(3)	2.906(3)
Na3-O1	2.566(8)	2.333(8)	2.866(8)	2.584(11)	2.409(12)	2.816(11)	2.590(15)	2.369(15)	2.822(15)	2.597(3)	2.402(3)	2.835(3)
Na3-O1	2.612(8)	2.353(8)	2.940(8)	2.614(11)	2.382(10)	2.889(11)	2.621(15)	2.371(15)	2.893(15)	2.632(3)	2.402(3)	2.906(3)
Na3-O1	2.568(8)	2.333(8)	2.866(8)	2.587(11)	2.409(12)	2.816(11)	2.592(15)	2.369(15)	2.822(15)	2.600(3)	2.402(3)	2.835(3)
Na3-O1	2.903(8)	2.585(8)	3.220(8)	2.947(11)	2.625(11)	3.239(11	2.955(15)	2.614(15)	3.239(15)	2.959(3)	2.647(3)	3.244(3)
Na3-O2	2.551(7)	2.509(7)	2.606(7)	2.606(10)	2.546(10)	2.673(10)	2.608(13)	2.537(13)	2.679(13)	2.615(2)	2.566(2)	2.673(2)
Na3-O2	2.652(8)	2.387(8)	2.928(8)	2.672(11)	2.442(11)	2.908(11)	2.671(8)	2.435(8)	2.900(8)	2.6754(16)	2.4557(16)	2.9071(16)
Na3-O2	2.647(8)	2.387(8)	2.928(8)	2.668(11)	2.442(11)	2.908(11)	2.666(8)	2.435(8)	2.900(8)	2.6711(16)	2.4557(16)	2.9071(16)
C-O1 x2	1.278(6)	1.252(6)	1.297(6)	1.275(7)	1.266(7)	1.284(6)	1.275(10)	1.257(10)	1.292(10)	1.281(3)	1.274(3)	1.286(3)
C-O1	1.278(6)	1.252(6)	1.297(6)	1.274(7)	1.266(7)	1.284(6)	1.275(10)	1.257(10)	1.292(10)	1.281(3)	1.274(3)	1.286(3)
C-O2	1.280(3)	1.274(3)	1.291(3)	1.273(4)	1.267(4)	1.277(4)	1.276(4)	1.272(4)	1.282(4)	1.283(2)	1.278(2)	1.288(2)

with respect to the room-temperature structure (Fig. 6). Thus, the second coordination sphere for C for the *Kh* crystal at 120 K would be better interpreted as 7–6 (and not 6–7 as at 293 K). This structural feature could be due to the minor presence of H replacing Na at the Na sites. Hydrogen, indeed, could slightly increase the flexibility of the graphite-like layer, thus hindering the stabilization of the commensurate structure. Since the variations of the CN of the C atoms are directly related to the incommensurate-commensurate phase transition (γ → δ phase transition), it can be postulated that in the natural natrite specimens studied here, the low-temperature commensurate structural state (δ phase—with coefficients of the modulation **q** vector: α = 1/6 and γ=1/3) could be stabilized only at temperatures lower than 120 K. Additional work at ultra-low temperatures (helium-cryostat) will be necessary to confirm this hypothesis.

A final interesting remark concerns the CO_3 group. This group seems to be a completely rigid unit in the average structure (Zubkova et al. 2002). However, the C-O distances and the C-3O torsion angle are slightly modulated along *t* (Fig. 7). At room temperature, the largest modulation of the C-O distances, 1.26(1)–1.29(1) Å, is observed in *Lv* for C-O1. The magnitude of this modulation is further increased with decreasing temperature: the C-O1 distance, indeed, changes from 1.252(6) to 1.297(6) Å in *Kh* at 120 K (Table 3; Fig. 7). The reasons of such a modulation have been described in detail by Arakcheeva and Chapuis (2005) for synthetic Na_2CO_3. A small deviation of the C-O2-O1-O1 torsion angle from 0° (Fig. 7) should be also mentioned. This deviation is negligible in *Lv* and in synthetic Na_2CO_3, but it reaches a value of about 1° in *Kh* at both 293 and 120 K. All C-O distances being restricted as equal to the average value, 1.279 Å for *Kh* (120 K) and 1.274 Å for *Kh* (293 K), make a planar CO_3 group. These restrictions do not significantly affect the *R* factors of the corresponding refinements. However, the ADPs of oxygen essentially increase, especially for the O1 atom: U_{eq} changes from 0.0186(3) to 0.0252(3) Å^2 for *Kh* (120 K) and from 0.0310(4) to 0.0481(5) Å^2 for *Kh* (293 K). This observation confirms the positional displacements of O atoms, resulting in the small distortions of the CO_3 group. Hence, the CO_3 group cannot be described as fully planar.

ACKNOWLEDGMENTS

This work has been performed with the support of the Swiss National Science foundation, (grant no. 20-105325/1 and 200021-109470/1), which is gratefully acknowledged. L.B. thanks M.I.U.R., P.R.I.N. 2007, project "Complexity in minerals: modulation, phase transition, structural disorder" issued to Silvio Menchetti. We are grateful to Marc-Olivier Diserens and Peter O. Baumgartner (SEM/EDXS laboratory, Institute of Geology and Paleontology, UNIL, Lausanne) for the help with the SEM facilities.

REFERENCES CITED

Arakcheeva, A. and Chapuis, G. (2005) A reinterpretation of the phase transitions in Na_2CO_3. Acta Crystallographica, B61, 601–607.

Arakcheeva, A., Pattison, P., Meisser, N., Chapuis, G., Pekov, I., and Thélin, P. (2007) New insight into the pectolite–serandite series: a single crystal diffraction study of $Na(Ca_{1.73}Mn_{0.27})[HSi_3O_9]$ at 293 and 100 K. Zeitschrift für Kristallographie, 222, 696–704.

Bindi, L., Bonazzi, P., Dušek, M., Petříček, V., and Chapuis, G. (2001) Five dimensional structure refinement of natural melilite $(Ca_{1.89}Sr_{0.01}Na_{0.08}K_{0.02})(Mg_{0.92}Al_{0.08})(Si_{1.98}Al_{0.02})O_7$. Acta Crystallographica, B57, 739–746.

Brouns, E., Visser, J.W., and de Wolff, P.M. (1964) An anomaly in the crystal structure of Na_2CO_3. Acta Crystallographica, 17, 614.

de Pater, C.J. and Helmholdt, R.B. (1979) Incommensurate structural phase transformation in Na_2CO_3. Physical Review B, 19, 5735–5745.

de Wolff, P.M. and Tuinstra, F. (1986) Incommensurate Phases in Dielectrics, 2, p. 253–281. Elsevier, Amsterdam.

Dušek, M., Chapuis, G., Meyer, M., and Petříček, V. (2003) Sodium carbonate revisited. Acta Crystallographica, B59, 337–352.

Janssen, T., Janner, A., Looijenga-Vos, A., and de Wolff, P.M. (2004) International Tables for Crystallography, Vol. C. In E. Prince, Ed., Mathematical, Physical and Chemical Tables, p. 907–945. Kluwer Academic Publishers, Dordrecht.

Janssen, T., Chapuis, G., and de Boissieu, M. (2007) Aperiodic Crystals: From modulated phases to quasicrystals. Oxford University Press, U.K.

Khomyakov, A.P. (1982) Natrite, Na_2CO_3—A new mineral. Zapiski Vsesouznogo Mineralogicheskogo Obchestva, 111, 220–225 (in Russian).

Petříček, V., Dušek, M., and Palatinus, L. (2000) Jana2000 Structure Determination Software Programs. Institute of Physics, Praha, Czech Republic.

Sass, R.L. and Scheuerman, R.F. (1962) The crystal structure of sodium bicarbonate. Acta Crystallographica, 15, 77–81.

van Aalst, W., den Hollander, J., Peterse, W.J.A.M., and de Wolff, P.M. (1976) The modulated structure of γ-Na_2CO_3 in a harmonic approximation. Acta Crystallographica, B32, 47–58.

Zubkova, N.V., Pushcharovsky, D.Yu., Ivaldi, G., Ferraris, G., Pekov, I.V., and Chukanov, N.V. (2002) Crystal structure of natrite, γ-Na_2CO_3. Neues Jahrbuch für Mineralogie, Monatshefte, 85–96.

MANUSCRIPT RECEIVED AUGUST 26, 2009
MANUSCRIPT ACCEPTED NOVEMBER 10, 2009
MANUSCRIPT HANDLED BY HONGWU XU